



# Extraction of Respiratory Signals and Respiratory Rates from the Photoplethysmogram

Shenglang Xiao<sup>1</sup>, Pengfei Yang<sup>1</sup>(✉), Luyao Liu<sup>2</sup>, Zhiqiang Zhang<sup>3</sup>, and Jiankang Wu<sup>4</sup>

<sup>1</sup> Xidian University, Xi'an 710071, Shaanxi, China

slxiao@stu.xidian.edu.cn, pfyang@xidian.edu.cn

<sup>2</sup> University of Science and Technology Beijing, Beijing 100083, China

17888841360@163.com

<sup>3</sup> University of Leeds, Leeds LS2 9JT, UK

Z.Zhang3@leeds.ac.uk

<sup>4</sup> University of Chinese Academy of Sciences, Beijing 100049, China

jkwu@ucas.ac.cn

**Abstract.** Respiration rate (RR) is an important indicator of human health assessment which can be estimated by extracting respiratory signals from the photoplethysmogram (PPG). The goal of this study is to propose an alternative method, for obtaining accurate estimation of respiratory rate (RR) from the PPG signal. The proposed algorithm is based on the multiple autoregressive models and autocorrelation analysis (AC-AR). In AC-AR, the autoregressive model (AR) is applied to determining the dominant respiratory rate from the PPG, and autocorrelation is applied to reduce the effect of clutter in the three respiratory-induced variations. Meanwhile, this paper introduced signal quality indices (SQI) to improve reliability of results. This algorithm is tested using an open source database: The CapnoBase benchmark dataset, which comprising 42 eight-minute PPG recording and respiratory signal acquired from both children and adults in different clinical setting. Compared with that of existing method in the literature, the average absolute error percentage (AAEP) of the proposed algorithm is less than 3.72%, which demonstrated that our presented AC-AR bring a significant improvement in accuracy.

**Keywords:** Respiratory rate (RR) · Photoplethysmography (PPG) · AR model · Data fusion

## 1 Introduction

Respiratory rate (RR) is one of the indicators used by hospitals to monitor patients for abnormal conditions, such as cardiac, respiratory arrest, systemic inflammatory response syndrome (SIRS), and renal failure [1]. Adults have a normal respiratory rate of 8–20 breaths per minute (bpm) [2]. In a study of respiratory abnormalities, 54% of cardiac

arrest patients had at least one  $RR > 27$  bpm three days before cardiac arrest [3]. Therefore, it is essential to monitor patients' respiratory. However, although pulse oximetry can be used to continuously measure heart rate (HR) and peripheral oxygen saturation (SpO<sub>2</sub>), continuous estimation of RR requires additional equipment, such as measurement of gas flow. Therefore, there is a need to improve the accuracy of RR estimates from the electrocardiogram (ECG), the photoplethysmogram (PPG) obtained from pulse oximeters [4, 5]. This paper focuses on extracting RR from PPG signals. Pulse oximeters estimate blood oxygen saturation (SpO<sub>2</sub>) based on Beer-Lambert's law, which indicates that the light intensity decays exponentially as it passes through the medium and the degree of attenuation is related to wavelength [6]. Therefore, we can use PPG to show the change in blood volume in the finger over time. The PPG signal includes a pulse component and a constant component, and the respiratory signal and the heartbeat signal are included in the pulse component [7].

The modulation of PPG signals by respiratory cycle includes a variety of ways, including amplitude modulation (AM), frequency modulation (FM), and baseline wander (BW) [8]. To extract the respiratory modulation signal from the PPG, the most common method is to detect the peak and trough of the PPG signal and obtain the respiratory modulation signal by calculation. In peak-trough detection in the time-domain, we define the time-series of peaks in the PPG to be a set of pairs  $\{t_{pk,i}, y_{pk,i}\}_{i=1\dots N_{pk}}$ , and the time-series of troughs in the PPG to be a set of pairs  $\{t_{tr,i}, y_{tr,i}\}_{i=1\dots N_{tr}}$ , where  $N_{pk}$  and  $N_{tr}$  are the number of peaks and troughs, respectively.  $N_{pk} \neq N_{tr}$  will be caused by noise in the signal or misdetection of the detection algorithm [6, 9, 10]. The time-series of peak and trough will be used to derive three different respiration-modulated signals, representing three different kinds of information about respiration [6]. (1) Respiration leads to change in cardiac output, causing respiratory-induced amplitude variation (RIAV), that is, change in peripheral pulse intensity. RIAV is defined as the height difference between two adjacent peaks and troughs. Therefore,  $y_{RIAV} = \{t_i, y_{pk,i} - y_{tr,i}\}_{i=1\dots N_{tr}}$ . (2) Respiration causes periodic changes in heart rate, namely respiratory-sinus arrhythmia (RSA). It appears that the heart rate increases during inhalation and decreases during exhalation, thereby causing respiratory-induced frequency variation (RIFV), which is defined as the time interval between successive PPG peaks. Therefore,  $y_{RIFV} = \{t_i, t_{i+1} - t_i\}_{i=1\dots N_{pk}}$ . (3) Respiration causes change in the pressure in the chest, causing blood exchange between the pulmonary and systemic circulation. Leading to a change in the baseline of perfusion, called respiratory induced intensity variation (RIIV). RIIV appears as the change in the amplitude of the peak of PPG waveform. Therefore,  $y_{RIIV} = \{t_i, y_{pk,i}\}_{i=1\dots N_{pk}}$ . There are also other respiratory modulation signals, such as pulse width variability [11], which can be used to estimate the RR (see Fig. 1).

Respiration modulates the PPG in different ways. Different methods of modulation signal extraction have been proposed in a number of literatures, which are discussed in Sect. 2. In Sect. 3, the improved Incremental-Merge Segmentation (IMS) algorithm and peak detection algorithm are introduced, and a combined algorithm for spectral analysis is proposed to improve the accuracy of RR estimation. Databases and evaluation methods are described in Sect. 4. Section 5 shows the results of RR estimation using the proposed algorithm. The significance and results of this study are discussed in Sect. 6.

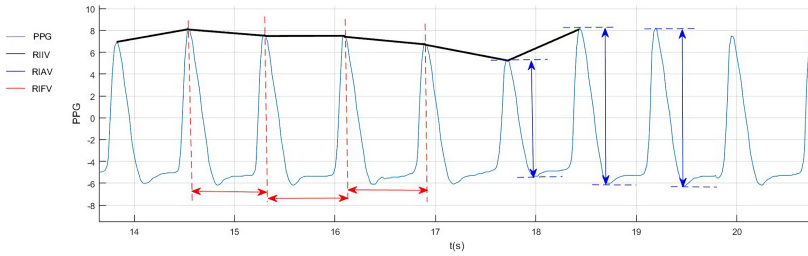


**Fig. 1.** PPG waveform and three respiration modulation signals. RIIV is the change in the baseline of perfusion; RIAV is the change in peripheral pulse intensity; RIFV is periodic changes in heart rate.

## 2 Related Work

Different algorithms have been proposed to estimate RR from PPG, such as digital filters [12], fast Fourier transforms (FFT) [6], wavelet decomposition [13] and hidden semi-Markov model [14]. Autoregressive model (AR) [9, 15], principal component analysis (PCA) [16] and artificial neural network (NN) [17], have all been successfully applied to various PPG databases with good estimation results. Some studies use neural networks to analyze the three modulation signals to select the best waveform for the algorithm design. There are also studies that use data fusion to combine estimates of multiple modulation signals [6, 18]. However, these methods have higher requirements for time domain waveforms. This problem can be solved by autocorrelation analysis. Autocorrelation analysis is a mathematical tool for finding repetitive patterns, such as periodic signals masked by noise. Since the respiratory signal can be viewed as a noisy periodic signal, the autocorrelation analysis can be used to calculate the respiratory rate [19]. In the autocorrelation signal, each peak (except the first) represents a period of strong autocorrelation, and the period with the greatest correlation can be regarded as the RR.

In order to extract effective information from chaotic PPG signal, researchers have proposed various methods. Byung S. Kim et al. used independent component analysis (ICA) to reduce motion artifact [16]. Despite so many advances, the use of pulse oximeters to measure respiratory rate has only recently been used commercially, because there are more reliable methods of RR estimation in clinical settings, such as spirometry or capacitance. Therefore, it is important to come up with a reliable method for PPG. A common method now is to introduce the signal quality index (SQI) to evaluate the signal quality [20]. If the PPG signal does not carry meaningful physiological information, it will not be algorithmically estimated. The lack of quality indicators may lead to serious clinical errors, and the introduction of evaluation indicators can improve accuracy and reliability.

To overcome this limitation, we designed an algorithm that uses all available respiratory-induced waveform to achieve significant accuracy. In this study, we propose an algorithm that combines the results of the three respiratory-induced variations described above, and use the AC-AR algorithm to estimate respiratory rate.

### 3 Proposed Algorithm

As for RR estimation, the most essential is the extraction of respiratory modulation signals. The main methods for extracting respiratory modulation signals are peak detection and signal quality assessment. Before the peak detection, the pre-processing procedure should be carried out first. A high-pass filter is applied to remove the dc component of the PPG signal. Then the PPG is segmented into pulses using IMS algorithm and artifacts are detected which are used to calculate signal quality (see Fig. 2). If the assessed quality is low, the RR estimation is not provided. This paper proposes an improved method for peak detection and signal evaluation, and then uses spectrum analysis and data fusion to estimate respiratory rate. In the following sections, we will describe RR estimation in more detail.

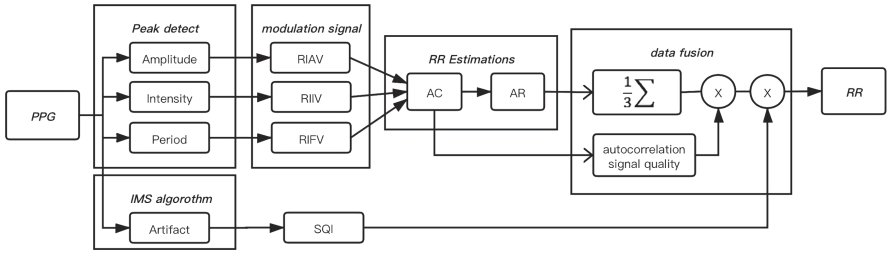


Fig. 2. The AC-AR algorithm flowchart.

#### 3.1 Peak Detection

The general principle of peak detection is that any singular point of a differentiable signal corresponds to a zero-crossing point or two inflection points in its derivative signal. This paper proposes a new method for peak detection (see Fig. 3). This method does not need to solve the second derivative, also does not need to solve the inflection point of the first derivative. Therefore, the computational efficiency can be improved to facilitate real-time processing. The specific method is shown in the *Algorithm 1* below. In order to avoid the impact of PPG signal amplitude changes on peak detection and verification, a 10 s sliding window is used for PPG waveform with an overlap time of 5 s.

In order to improve detection accuracy, peak verification is needed which mainly considers two factors, the amplitude threshold and the time interval threshold. The method of setting the amplitude threshold is shown below. Let  $\text{thresh1}$  be the ninth decile and  $\text{thresh2}$  be the first decile. Then,

$$\text{thresh3} = \text{thresh2} + 0.7 * (\text{thresh1} - \text{thresh2}) \quad (1)$$

and then,

$$\text{highdiff} = \text{abs}(\text{peaks} - \text{thresh1}) \quad (2)$$

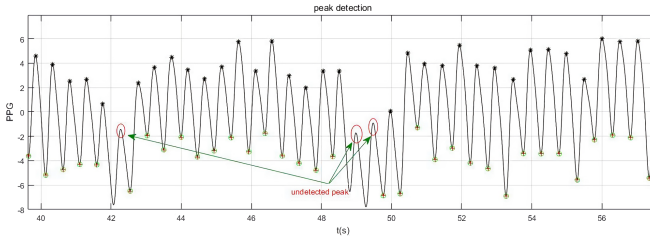


**Fig. 3.** The result of peak detection algorithm

$$\text{middlediff} = \text{abs}(\text{peaks} - \text{thresh3}) \tag{3}$$

$$\text{lowdiff} = \text{abs}(\text{peaks} - \text{thresh2}) \tag{4}$$

where *peaks* is the time-series of peaks. If condition

$$(\text{highdiff} < \text{middlediff}) \& (\text{highdiff} < \text{lowdiff}) \tag{5}$$

is met, the peak point is recorded.

---

**Algorithm 1** Peak detection algorithm

---

- 1:  $\text{data} \leftarrow \text{PPG}$ ;
  - 2:  $\text{diff} \leftarrow \text{diff}(\text{data})$ ;
  - 3:  $\text{left\_diff} \leftarrow \text{diff}[1: \text{end}-1]$ ;
  - 4:  $\text{logical\_left} \leftarrow \text{logical}(\text{left\_diff} > 0)$ ;
  - 5:  $\text{right\_diff} \leftarrow \text{diff}[2: \text{end}]$ ;
  - 6:  $\text{logical\_right} \leftarrow \text{logical}(\text{right\_diff} > 0)$ ;
  - 7:  $\text{peaks} \leftarrow \text{find}(\text{logical\_left} \& \text{logical\_right} = 1) + 1$ ;
- where  $\text{diff}(X)$  calculates the difference between  $X$  adjacent elements along the first array dimension whose size is not equal to 1;  $\text{logical}(A)$  converts  $A$  to an array of logical values. Any non-zero element in  $A$  will be converted to the logical value 1 (true), and zero to the logical value 0 (false);  $\text{find}(X)$  returns a vector containing a linear index of each non-zero element in the array  $X$ .
- 

In terms of time interval, because the pulse wave is mainly regulated by the heartbeat, and the normal person’s resting heart rate is 60–100 bpm, the peak of the time interval corresponding to this range will be detected. For trough detection, the PPG waveform shows that the minimum value between two peaks is the trough. The time-series of peak and trough will be used to derive three different respiration-modulated signals, representing three different kinds of information about respiration.

### 3.2 Signal Quality Index

Since there are motion artifacts and noise that cannot be filtered out in the PPG, the quality of the PPG needs to be evaluated. The signal quality evaluation method used in this paper is analyzed for consistency. First, the PPG pulse is divided into line segments

using Incremental-Merge Segmentation (IMS) algorithm. According to the shape of the line segment, it is distinguished into effective signals and noise. This paper calculates the ratio of artifact and clip in the signal as the SQI for the signal quality.

The IMS algorithm can be used for real-time processing with a sliding window structure [21]. The algorithm only needs to set a parameter  $m$  (the number of points moved each time, mainly related to the sampling rate). The principle is to divide the PPG signal into  $n$   $m$ -length segments, calculate the slopes of these segments, and merge them with the same slope, and the different slopes are divided into new Line segments. After the IMS algorithm, each PPG pulse is represented as a straight line from the beginning of the pulse to the end of the primary peak of the pulse (see Fig. 4).

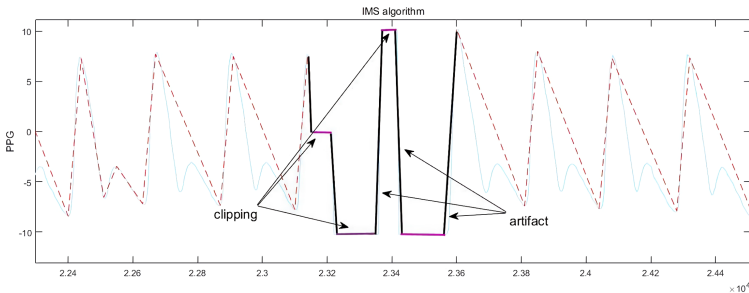


**Fig. 4.** The result of IMS algorithm and Artifact detection

Since the upslope and downslope line segments have a one-to-one correspondence, the upslope line segments are analyzed separately. If the amplitude and slope of the upslope line segment both exceed the threshold, it is regarded as artifact; if the slope is zero, it is regarded as clip; the line segment immediately after the clip is also artifact. SQI is calculated according to the ratio of artifact and clip in the PPG for signal quality. If the SQI is less than the threshold, then the data window is labeled as low RR estimation quality (see Fig. 5).

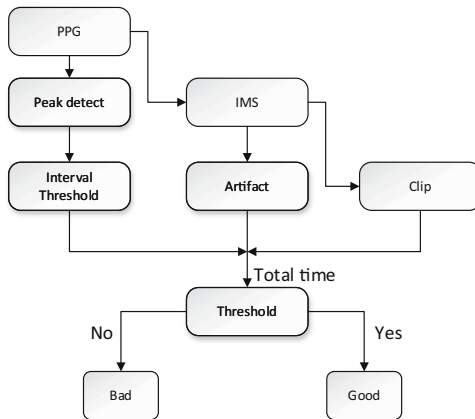


**Fig. 5.** SQI algorithm flowchart

### 3.3 Estimation of Respiratory Rate

After the time-series of peak and trough are obtained from the peak detection, the above method is used to calculate three kinds of respiratory modulation signals: RIIV, RIFV, and RIAV. Because these modulation signals are unevenly-sampled time-series, they are resampled at  $f_s = 4$  Hz, using linear interpolation. Each resampled time-series is normalized using a zero-mean unit-variance transformation, so that the amplitudes of the three modulation signals are unified to the same range for subsequent spectral analysis. Then use a high-pass filter to remove the low-frequency signal, and a moving average filter to smooth the signal. The next step is to extract the respiratory rate.

**Autocorrelation Analysis.** Autocorrelation analysis is a mathematical tool for finding repetitive patterns, such as periodic signals masked by noise. Since the respiratory signal can be viewed as a noisy periodic signal, the autocorrelation analysis can be used to calculate the respiratory rate. The autocorrelation formula is as follows,

$$\rho_x(\tau) = \frac{E[(x_i - \mu)(x_{i+\tau} - \mu)]}{\sigma^2} \tag{6}$$

where  $x_i$  is the time-series of signal,  $x_{i+\tau}$  is the time-series translated by  $\tau$  units,  $\mu$  is the mean, and  $\sigma^2$  is the variance. An autocorrelation sequence  $C[\tau]$  can be combined by the value of formula from  $\tau = 0$  to  $\tau = n - 1$ . In the autocorrelation signal, each peak (except the first) represents a period of strong autocorrelation, and the period with the greatest correlation can be regarded as the RR. Therefore, we can use autocorrelation analysis to obtain the periodicity of the respiratory signal.

We apply the autocorrelation to analyze the signal as Fig. 6 shows. As the result, the autocorrelation coefficient waveform contains the breath rate signal, and it overcomes the effect of noise and clutter. At last, we can analyze these coefficients by AR model to acquire the more accurate RR.

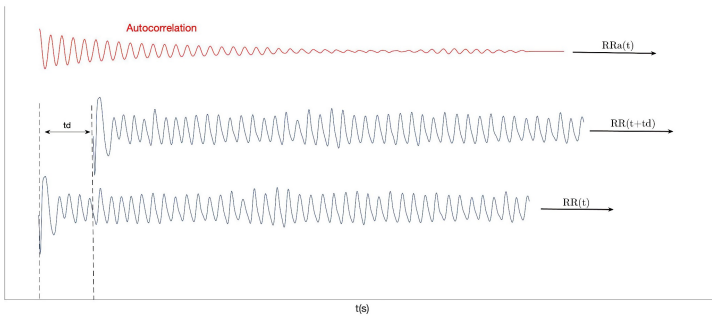


**Fig. 6.** Autocorrelation analysis diagram

**AR Model.** AR model is an alternative to the discrete Fourier transform (DFT) and one of the methods for high-resolution spectral estimation of short-term sequences. In

biomedical engineering, AR models are widely used for spectrum analysis of heart rate variability and electroencephalography analysis. In AR model, each point in the time-series is a regression of its past points. The number  $M$  of past points used is called the order of AR model. AR model can be regarded as a filter, which divides the time-series into predictable time series and prediction error series. Compared with the DFT, it provides a smoother and more intuitive power spectrum, and yet is more complicated. The AR model is defined as,

$$x[n] = \sum_{i=1}^M a_i x[n-i] + \varepsilon[n] \quad (7)$$

where  $M$  is the model order,  $a_i$  is the weight, and  $\varepsilon[n]$  is the prediction error and follows  $\varepsilon \sim N(0, \sigma)$ . The least squares method is used to minimize the prediction error  $\varepsilon[n]$  to obtain the optimal parameter  $a_{opt}$ . Matrix the above formula,

$$x = Xa + \varepsilon \quad (8)$$

when the prediction error  $\varepsilon[n]$  reaches the minimum, the parameter  $a_{opt}$  is optimal, that is,

$$\varepsilon = x - Xa_{opt} = 0 \quad (9)$$

$$X^T \varepsilon = X^T (x - Xa_{opt}) = 0 \quad (10)$$

$$X^T x = X^T X a_{opt} \quad (11)$$

$$\left(X^T X\right)^{-1} \left(X^T X\right) a_{opt} = a_{opt} = \left(X^T X\right)^{-1} X^T x \quad (12)$$

Another point of AR model is the choice of model order  $M$ . Different orders have different effects in AR model. In practice, by fitting the sequence to multiple orders, the order with the best effect is selected. The most common selection criterion is Akaike's Information Criterion (AIC),

$$AIC(M) = N \cdot \ln(\sigma_p^2) + 2M \quad (13)$$

where  $\sigma_p^2$  is the variance of the prediction error  $\varepsilon[n]$ . The best model order is  $M$  that minimizes AIC.

Then, the time-series spectrum  $R(e^{j\omega})$  can be obtained by multiplying the square of the transfer function and the variance of the prediction error,

$$R(e^{j\omega}) = \left| H(e^{j\omega}) \right|^2 \sigma_p^2 \quad (14)$$

where  $H(e^{j\omega})$  is the transfer function of AR model,

$$H(e^{j\omega}) = \frac{1}{1 - a_1 e^{-j\omega} - \dots - a_M e^{-jM\omega}} \quad (15)$$

The autocorrelation method can remove the noise in the periodic signal with the characteristics described above. Each peak of the autocorrelation sequence represents a period of strong autocorrelation, so the period of the autocorrelation corresponds to the period of the original signal. Therefore, the autocorrelation signal of the respiratory modulation signal used as the input signal of AR spectrum analysis to estimate the RR.

### 3.4 Data Fusion

In order to improve the accuracy and reliability of RR estimation, data fusion can be performed on three kinds of respiratory modulation signals. A common fusion method is to average the spectrum of the three kinds of modulation signals, and the maximum value is selected as RR. This paper proposes an improvement method.

Due to the autocorrelation signal of the modulation signal can be analyzed as a breathing signal, and the waveform of the autocorrelation signal is more regular. First use the IMS algorithm to segment the autocorrelation signal. Since the autocorrelation signal of a normal breathing signal is approximately a sine wave, its variance value is small, and its mean value is close to 1, that is, the waveform is relatively stable (see Fig. 7). An analysis of variance is performed on the autocorrelation signal, and autocorrelation signal quality (ASQ) is used as an indicator,

$$\text{ASQ} = \text{var}/\text{mean} \quad (16)$$

where var is the variance of these line segments, and mean is the mean of these line segment. The spectrums of the modulation signal with ASQ less than a certain range are processed by average.

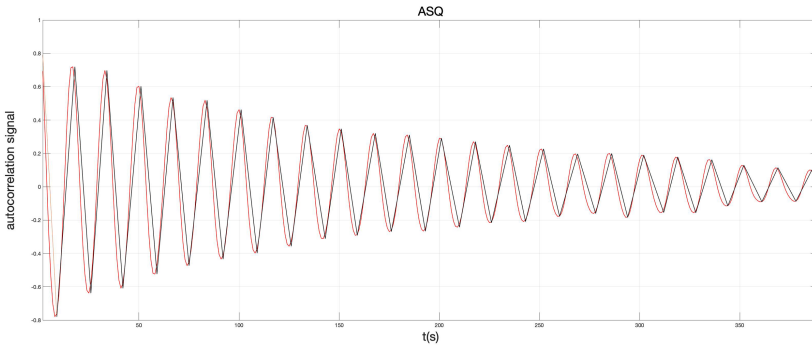


Fig. 7. Autocorrelation signal quality

## 4 Materials and Methods

The method was implemented and tested using the MATLAB software framework, v.R2018a (Mathworks, Natick, MA, USA), and it was designed to be used on each single window (independently of the others). An open-source dataset, the CapnoBase benchmark dataset (available at [www.capnobase.org](http://www.capnobase.org)) was used for the analysis described in this paper. The database which contained PPG signals, ECG signals, and respiratory signals was collected by Karlen et al. The sampling frequency was 300 Hz. These data were collected from 59 children (mean age 8.7) and 35 adults (mean age 52.4). The author of the database randomly selects a part of it, and then combines it into a new data set, which contains 42 data segments with a duration of 8 min. Each recorded CO<sub>2</sub>

tracing waveform was used as a reference “gold standard” record for RR. Each breath on the carbon dioxide map in the database has been manually marked by the research assistant, and the reference RR value is derived based on the average time between two consecutive breaths using annotations [6].

Before data analysis, preprocessing is performed. We remove the linear trend of the signal to avoid errors caused by data offset and then use low-pass filtering to remove high-frequency noise. The three methods mentioned above are then used to extract the respiratory modulation signal. The signals are resampled since they are unevenly-sampled time-series. Each resampled time-series is normalized using a zero-mean unit-variance transformation. In order to increase the reliability of the signal, a signal evaluation index (SQI) is introduced to evaluate the quality of the modulated signal. In this study, RR was estimated to be within a reasonable range of breathing frequencies set at 4 to 65 breaths per minute.

To extract the RR from the PPG, a common method is to use a sliding window to segment the PPG time-series, and each window obtains an RR. This experiment uses two windows size of 30 s and 60 s, and estimates the RR every 3 s and 6 s, respectively. Based on the estimated value and the reference value, performance was assessed by calculating the mean absolute error (MAE) and average absolute error percentage (AAEP) in breaths per minute for each record, defined as,

$$\text{MAE} = \frac{1}{w} \sum_{i=1}^w |y_i - y_{ref,i}| \quad (17)$$

$$\text{AAEP} = \frac{1}{w} \sum_{i=1}^w \frac{|y_i - y_{ref,i}|}{y_{ref,i}} \quad (18)$$

where  $w$  is the number of reference value,  $y_i$  is estimate value, and  $y_{ref,i}$  is reference value. The observation value of each algorithm is compared with the reference observation value, and the measurement error of the observation value of each algorithm is calculated. The first 64 s are not used for performance measurements because they are used to initialize high-pass filters and sliding window. All RR estimation methods, including the single modulation methods, ignore the measurement errors of the windows containing artifacts automatically detected by the algorithm.

## 5 Results

According to the experiment, for the signal with a sampling frequency of 300 Hz, the IMS algorithm can obtain a better result when  $m = 10$ . It provides a good tradeoff between calculating load and time resolution for pulse peak detection. Different time windows have no significant effect on RR measurement errors, but larger windows can slow down the real-time response of the algorithm. But when the time window is too small, the lower respiratory rate cannot be detected. Therefore, we eclectically selected the time window of 60 s for analysis. Firstly, the PPG signal is analyzed from the time-frequency domain. Figure 8(a) is the PPG signal, and the spectrum analysis is shown in Fig. 8(b). From the frequency spectrum, we can find that the energy of the breath rate signal is weaker compared with the heart signal and its harmonics. Therefore, it is necessary to

extract the respiratory modulation signal from PPG signal to avoid the interference of heartbeat signal. As can be seen from Fig. 9, after using the AC-AR algorithm proposed in this paper, the spectrum is concentrated near RR.

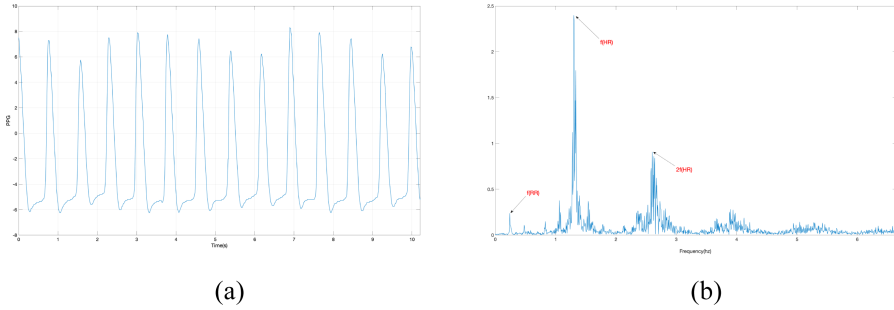


**Fig. 8.** PPG signal (a) and frequency spectrum (b)

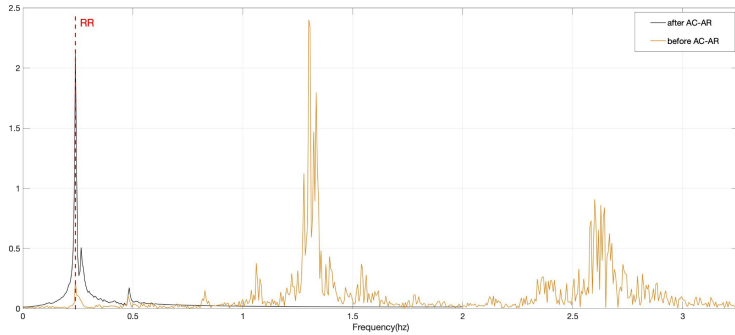


**Fig. 9.** The frequency spectrum of 180 s respiratory signal before AC-AR (yellow) and after AC-AR (black). The red dotted line is the respiratory rate. (Color figure online)

After signal preprocessing, we get the respiratory modulation signal from the PPG signal. Figure 10 shows the comparison between the reference respiratory signal and the respiratory modulation signal extracted using the peak detection algorithm proposed in this paper. The extracted respiratory signal is basically similar to the reference respiratory signal, which is of great help to the subsequent analysis. Following the signal processing method previously mentioned, respiratory rates are acquired through the AC-AR algorithm. By the above formula and reference respiratory rate, we can calculate the MAE and AAEP. From Table 1, we can see that the result is much improved after using SQI. In the CapnoBase database, some signals are chaotic, and the results with large errors will be obtained by using these signals to analyze. Using SQI can avoid these errors, which is beneficial to the reliability of clinical results. Meanwhile, compared with AR model, the AAEP of the AC-AR algorithm decreased by about 1%. From Table 2, the accuracy is improved to some extent after data fusion with ASQ, which proves that the feasibility

of data fusion using this method. Compared with averaging the spectrum directly, using ASQ can dynamically select a better spectrum as the result according to the quality of autocorrelation signal.

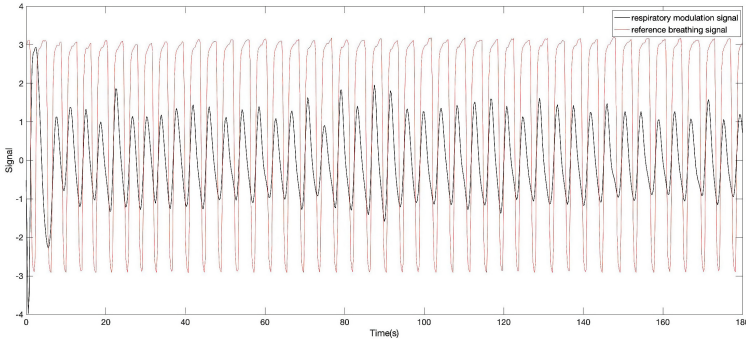


**Fig. 10.** Comparison of respiratory modulation signals with reference breathing signals. After processing, the respiratory signals can be extracted normally.

**Table 1.** Comparison of results

	AAEP	
	AC	AC-AR
Before using SQI	8.37%	7.56%
After using SQI	4.27%	3.72%

**Table 2.** The result of ASQ

	RIIV	RIFV	RIAV	ASQ
AAEP	6.61%	5.61%	8.55%	3.72%

As can be seen from the boxplot (see Fig. 11), the MAEs are quite different when using one of the modulation signals alone. The results of RIIV are obviously better than the other two, indicating that RIIV has the strongest modulation of PPG signal. After using data fusion and SQI, the experimental results are obviously better. Among them, the results of data fusion using ASQ were better than SQI analysis of single respiratory modulated signal, indicating that it is necessary to conduct quality analysis of modulated signal. Moreover, the result of data fusion using autocorrelation signal quality is better than that of spectrum averaging. Without considering the outliers, the error of the AC-AR algorithm is  $0.12 \pm 0.36$  bpm.

To further evaluate the algorithm, a scatter plot is drawn for analysis (see Fig. 12). Best Fit stands for PPG respiratory rate equal to the reference respiratory rate, and the

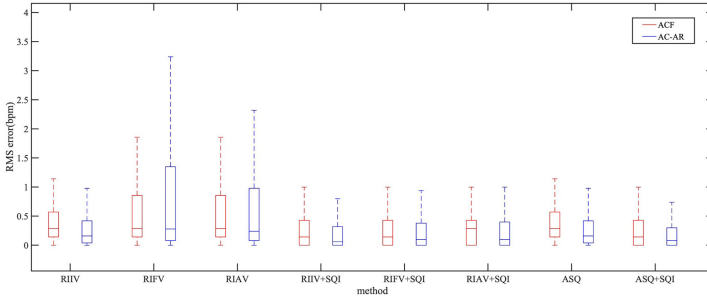


**Fig. 11.** Results for the CapnoBase benchmark dataset using 60 s windows. The boxplots give the RMS Error for the different RR estimation methods.

closer the vertical distance to the line, the better the result. As can be seen from the figure, results are concentrated near the Best Fit, indicating that the AC-AR algorithm identified and eliminated a majority of high error estimations. This also shows that the algorithm proposed in this paper is feasible and accurate.

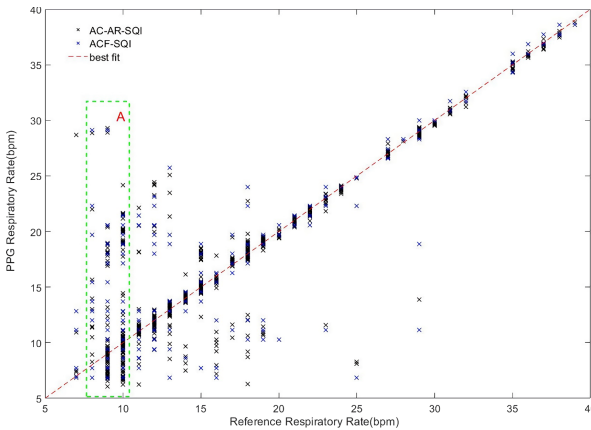


**Fig. 12.** Scatter plot comparing the reference RR obtained from capnometry with the PPG RR obtained from the ACF and AC-AR algorithm. The AC-AR eliminates the estimations with large error (distance from Best fit). Box A: The signal has been badly distorted.

## 6 Conclusion

In this paper, we improved the method of obtaining respiratory modulation signals and proposed a new analysis method that can be used in combination with other respiratory frequency analysis methods to improve the accuracy and robustness of respiratory frequency estimation. The autocorrelation method can remove noise in a periodic signal having the above characteristics. Each peak of the autocorrelation sequence represents

a period of strong autocorrelation, so the period of the autocorrelation corresponds to the period of the original signal. Autoregression (AR) model uses the time history of the signal to extract the important information hidden in the signal. Therefore, the autocorrelation signal of the respiratory modulation signal can be used as the input signal of AR spectrum analysis to estimate the RR. Several experiments have been performed on different datasets with different methods. The experimental results show that the average absolute error percentage (AAEP) is less than 3.72%. It is proved that the method of autocorrelation combined with autoregressive model used to extract respiratory rate from PPG is feasible and reliable. Finally, it can be seen from the boxplot that the result of each algorithm has a lot of outliers. The problem is that when the waveform of the PPG signal is relatively chaotic, the respiratory modulation signal extracted from it is not reliable. If the baseline drift of the PPG signal is severe, there will be errors in the peak detection results, which will cause some peaks to be missed. To solve this problem, our next goal is to better remove motion noise so that the respiratory rate can be extracted from people in motion.

## References

1. Van Leuvan, C.H., Mitchell, I.: Missed opportunities? An observational study of vital sign measurements. *Crit. Care Resuscitation* **10**(2), 111–115 (2008)
2. Hooker, E.A., et al.: Respiratory rates in emergency department patients. *J. Emerg. Med.* **7**(2), 129–132 (1989)
3. Birrenkott, D.A., Pimentel, M.A., Watkinson, P.J., Clifton, D.A.: A robust fusion model for estimating respiratory rate from photoplethysmography and electrocardiography. *IEEE Trans. Biomed. Eng.* **65**(9), 2033–2041 (2018)
4. Walsh, J.A., et al.: Novel wireless devices for cardiac monitoring. *Circulation* **130**(7), 573–581 (2014)
5. Hubner, P., et al.: Surveillance of patients in the waiting area of the department of emergency medicine. *Medicine* **94**(51), Article no. e2322 (2015)
6. Karlen, W., Raman, S., Ansermino, J.M., Dumont, G.A.: Multiparameter respiratory rate estimation from the photoplethysmogram. *IEEE Trans. Biomed. Eng.* **60**(7), 1946–1953 (2013)
7. Charlton, P.H., Birrenkott, D.A., Bonnici, T., Pimentel, M.A.F.: Breathing rate estimation from the electrocardiogram and photoplethysmogram: a review. *IEEE Rev. Biomed. Eng.* **11**, 2–20 (2018)
8. Birrenkott, D.: Respiratory quality indices for ECG- and PPG-derived respiratory data. D.Phil transfer of status report, Department of Engineering and Science, University of Oxford, Oxford, U.K (2015)
9. Pimentel, M.A.F., et al.: Toward a robust estimation of respiratory rate from pulse oximeters. *IEEE Trans. Biomed. Eng.* **64**(8), 1914–1923 (2017)
10. Meredith, D., et al.: Photoplethysmographic derivation of respiratory rate: A review of relevant respiratory and circulatory physiology. *J. Med. Eng. Technol.* **36**(1), 60–66 (2012)
11. Lázaro, J., Gil, E., Bailón, R., Mincholé, A., Laguna, P.: Deriving respiration from photoplethysmographic pulse width. *Med. Biol. Eng. Comput.* **51**, 233–242 (2013)
12. Nilsson, L., et al.: Monitoring of respiratory rate in postoperative care using a new photoplethysmographic technique. *J. Clin. Monit. Comput.* **16**(4), 309–315 (2000)
13. Leonard, P., et al.: An algorithm for the detection of individual breaths from the pulse oximeter waveform. *J. Clin. Monit. Comput.* **18**(5/6), 309–312 (2004)

14. Pimentel, M.A.F., Santos, M.D., Springer, D.B., Clifford, G.D.: Heart beat detection in multimodal physiological data using a hidden semi-Markov model and signal quality indices. *Physiol. Meas.* **36**, 1717–1727 (2015)
15. Takalo, R., Hytti, H., Ihalainen, H.: Tutorial on univariate autoregressive spectral analysis. *J. Clin. Monit. Comput.* **19**, 401–410 (2005)
16. Kim, B.S., Yoo, S.K.: Motion artifact reduction in photoplethysmography using independent component analysis. *IEEE Trans. Biomed. Eng.* **53**(3), 566–568 (2006)
17. Johansson, A.: Neural network for photoplethysmographic respiratory rate monitoring. *Med. Biol. Eng. Comput.* **41**, 242–248 (2003)
18. Khreis, S., Ge, D., Rahman, H. A., Carrault, G.: Breathing rate estimation using kalman smoother with electrocardiogram and photoplethysmogram. *IEEE Trans. Biomed. Eng.* **67**, 893–904 (2019)
19. Nguyen, N.T.P., Lyu, P., Lin, M.H., Chang, C., Chang, S.: A short-time autocorrelation method for noncontact detection of heart rate variability using CW doppler radar. In: 2019 IEEE MTT-S International Microwave Biomedical Conference (IMBioC), China, pp. 1–4 (2019)
20. Orphanidou, C., Bonnici, T., Charlton, P., Clifton, D., Vallance, D., Tarassenko, L.: Signal-quality indices for the electrocardiogram and photoplethysmogram: derivation and applications to wireless monitoring. *IEEE J. Biomed. Health Inf.* **19**(3), 832–838 (2015)
21. Karlen, W., Ansermino, J.M., Dumont, G.: Adaptive pulse segmentation and artifact detection in photoplethysmography for mobile applications. In: 34th Annual International Conference of the IEEE EMBS (2012)